International Journal of Nanomedicine

Dovepress
open access to scientific and medical research

Open Access Full Text Article

ORIGINAL RESEARCH

Enhanced antifungal efficacy of tebuconazole using gated pH-driven mesoporous nanoparticles

This article was published in the following Dove Press journal:
International Journal of Nanomedicine
23 May 2014
Number of times this article has been viewed

Núria Mas[1–3]
Irene Galiana[3]
Silvia Hurtado[†]
Laura Mondragón[1–3]
Andrea Bernardos[1–3]
Félix Sancenón[1–3]
María D Marcos[1–3]
Pedro Amorós[4]
Nuria Abril-Utrillas[5]
Ramón Martínez-Máñez[1–3]
José Ramón Murguía[1,3]

[1]Centro de Reconocimiento Molecular y Desarrollo Tecnológico (IDM), Centro Mixto Universidad Politécnica de Valencia, Universidad de Valencia, Valencia, Spain; [2]Departamento de Química, Universidad Politécnica de Valencia, Valencia, Spain; [3]CIBER de Bioingeniería, Biomateriales y Nanomedicina, Madrid, Spain; [4]Institut de Ciència del Materials (ICMUV), Universitat de València, Valencia, Spain; [5]Servicio Ginecología y Obstetricia, Hospital de la Plana, Vila-real, Spain

[†]Silvia Hurtado passed away in September 2013

Correspondence: José Ramón Murguía
Centro de Reconocimiento Molecular y Desarrollo Tecnológico (IDM), Centro Mixto Universidad Politécnica de Valencia, Universidad de Valencia, Camino de Vera s/n, 46022 Valencia, Spain
Tel +34 96 387 9416
Fax +34 96 387 9349
Email muribajo@ibmcp.upv.es

Ramón Martínez-Máñez
Centro de Reconocimiento Molecular y Desarrollo Tecnológico (IDM), Centro Mixto Universidad Politécnica de Valencia, Universidad de Valencia, Camino de Vera s/n, 46022 Valencia, Spain
Tel +34 96 387 7343
Fax +34 96 387 9349
Email rmaez@qim.upv

Abstract: pH-sensitive gated mesoporous silica nanoparticles have been synthesized. Increased extracellular pH and internalization into living yeast cells triggered molecular gate aperture and cargo release. Proper performance of the system was demonstrated with nanodevices loaded with fluorescein or with the antifungal agent tebuconazole. Interestingly, nanodevices loaded with tebuconazole significantly enhanced tebuconazole cytotoxicity. As alterations of acidic external pH are a key parameter in the onset of fungal vaginitis, this nanodevice could improve the treatment for vaginal mycoses.

Keywords: capped mesoporous nanoparticles, intracellular release, pH-responsive nanoparticles, *Saccharomyces cerevisiae,* tebuconazole loading

Introduction

Vaginitis is an inflammation of the vagina, often associated with irritation or infection of the vulva. Vulvovaginitis is very common and affects women of all ages. Indeed, 75% of all women will suffer from this condition at least once throughout their lives.[1] If left untreated, it can lead to further complications, especially for pregnant women. Infectious vaginitis can account for more than 90% of all vulvovaginitis cases. It is caused by either bacterial or, most frequently, Candida infections.[2]

Candida is among the normal organisms that are part of the commensal flora of the gut, mouth, and genital tract.[3] These yeasts will multiply when their habitat becomes altered under particular conditions, such as immunosuppression, administration of antibiotics, pregnancy, the luteal phase of the menstrual cycle, diabetes mellitus, or oral contraceptive intake.[3,4] As a consequence, Candida infection causes the elimination of beneficial micro-organisms from the endogenous vaginal flora (especially Döderlein's bacillus), one of the natural mechanisms of defense. Metabolism of lactobacillus present in the genital tract generates lactic acid, which is principally responsible for maintaining a normal vaginal pH around 3.8–4.4. This acid environment hinders the growth of other pathogenic micro-organisms acting as a protecting barrier. If there is an increase in the pH to values around 5.5–6.8, an overgrowth of Candida occurs, thus causing the most common vulvovaginal infections.[4]

Management of vaginal candidiasis includes oral or topical antibiotics and/or antifungal creams or similar medications.[4] Most of the available effective antifungal agents are based on polyenes (amphotericin B), triazoles (fluconazole, itraconazole), or echinocandins.[1,5] Although both oral and topical treatments are equally effective, oral therapies are strongly associated with systemic side effects. Topical therapies are less frequently associated with adverse effects, which include irritation, itching,

burning, and development of yeast resistance to antifungal agents.[5] Their better therapeutic profile, together with cost-effectiveness, makes topical therapies the option of choice for management of vaginal candidiasis.

Although silver[5,6] and silica nanoparticles[7] have been used as antifungals against *Candida* spp., we believe that the use of gated mesoporous materials could be an interesting alternative as drug carriers in order to avoid the mentioned adverse effects.

The development of nanoscopic hybrid materials able to deliver cargo under a certain external trigger action has been considered a highly interesting area of research and has been extensively explored in the last few years.[8,9] These nanodevices have been demonstrated to be an excellent approach for advanced controlled release research.[9–17] Gated mesoporous supports are composed basically of two subunits, a suitable scaffolding, and certain entities anchored on the support surface.[18] The support is employed as a container in which certain chemical species could be stored, whereas the grafted molecules in the outer surface of the scaffold act as a molecular gate, controlling the cargo release at will. The selection of both scaffold and anchored entities of the nanodevice has to be done carefully, given the required functionalities of the final system.

In this context, silica mesoporous supports are widely used as inorganic scaffolds, thanks to several favorable features, including homogeneous porosity, high chemical inertness, robustness, thermal stability, high loading capacity, biocompatibility, and ease of functionalization through the well-known chemistry of alkoxysilanes.[19–28] Although mesoporous silica supports have been used for the simple diffusion-controlled release of certain antibiotics[29–31] and antifungals,[4,32] similar studies using capped materials showing zero release and able to deliver cargo only in the presence of fungi have not been described.

We aimed to design and test a new nanodevice for the intracellular controlled release of an antifungal in opportunistic fungi, such as *Candida* spp., reproducing the biological conditions of the vagina ecosystem. When growing in the yeast form, *Candida albicans* is morphologically similar to *Saccharomyces cerevisiae*,[33] validating budding yeast as a model for fungal infections.[34] Furthermore, *S. cerevisiae* itself can also cause vaginal yeast infections.[35] We hypothesize that apart from the increase of the vaginal pH under certain conditions, nanoparticle internalization in budding yeast would trigger the opening of the nanodevice and the release of the entrapped antifungal molecule. This would be so because at pH <5 the amine groups are protonated and the electrostatic repulsions between the organic moieties and the interaction with anions in the medium maintains the gate closed. At pH >5 the amine groups are less protonated, weakening the electrostatic interactions and causing opening of the gate, which is followed by a massive outflow of the entrapped moieties.[36,37]

Material and methods

Chemicals

The chemicals tetraethyl orthosilicate (TEOS) (98%), n-cetyltrimethylammonium bromide (CTAB) (≥99%), sodium hydroxide (≥98%), fluorescein (FL), tebuconazole, and 3-[2-(2-aminoethylamino)ethylamino]propyltrimethoxysilane (N3) were provided by Sigma-Aldrich (St Louis, MO, USA). The culture yeast was also provided by Sigma-Aldrich. Solvents were purchased from Scharlab, SA (Barcelona, Spain). All reagents were used as received.

General techniques

Powder X-ray diffraction (PXRD), thermogravimetry analysis (TGA), elemental analysis, transmission electron microscopy (TEM), and nitrogen adsorption–desorption techniques were employed to characterize the prepared materials. PXRD measurements were performed on a Philips D8 Advance Diffractometer using Cu Kα radiation. TGA was carried out on a TGA/SDTA 851e Mettler-Toledo S.A.E. (Barcelona, Spain) balance using an oxidant atmosphere (air, 80 mL/minute) with a heating program consisting of a heating ramp of 10K per minute 393–1,273 K and an isothermal heating step at this temperature for 30 minutes. Elemental analysis was performed in a CE Instrument EA-1110 CHN Elemental Analyzer. TEM images were obtained with a 100 kV JEOL JEM-1010 microscope (JEOL, Tokyo, Japan). Nitrogen adsorption–desorption isotherms were recorded on a Micromeritics ASAP2010 (Bonsai Advanced Technologies SL., Madrid, Spain) automated sorption analyzer. The samples were degassed at 120°C in a vacuum overnight. The specific surface areas were calculated from the adsorption data in the low pressures range using the Brunauer–Emmett–Teller (BET) theory model.[38] Pore size was determined following the Barrett–Joyner–Halenda (BJH) method.[39] Fluorescence spectroscopy was carried out on a Felix 32 Analysis Version 1.2 (Build 56) (Microbeam SA, Barcelona, Spain). Yeast cultures were inoculated in a Telstar AH100 (Madrid, Spain) cell culture hood, grown at 30°C using a microbiology culture shaker (Kühner 25 mm; Adolf Kühner AG, Basel, Switzerland), and monitored under microscopy with a Nikon Eclipse E500 (Nikon Instruments Europe B.V. Amsterdam, the Netherlands).

Synthesis of the nanoparticles

Synthesis of the silica support

The MCM-41 (mobil composition of matter-41) mesoporous nanoparticles were synthesized by the following procedure: CTAB (1.00 g, 2.74 mmol) was first dissolved in deionized water

(480 mL). After that, NaOH (3.5 mL, 2.00 M) in deionized water was added to the CTAB solution. Next, the solution temperature was adjusted to 80°C. TEOS (5.00 mL, 2.57×10^{-2} mol) was then added dropwise to the surfactant solution. The mixture was stirred for 2 hours to yield a white precipitate. Finally, the solid product was centrifuged, washed with deionized water and ethanol, and dried at 60°C (MCM-41 as synthesized). To prepare the final porous material (MCM-41), the as synthesized solid was calcined at 550°C using an oxidant atmosphere for 5 hours in order to remove the template phase, (CTAB), thus eliminating any residual CTAB that might negatively affect cell viability.

Synthesis of MCM-41 loaded with tebuconazole (S1-Teb)

In a typical synthesis, template-free MCM-41 (150 mg) was suspended in a solution of tebuconazole (16 mg in 7 mL of CH_2Cl_2 for a ratio of 0.35 mmol of tebuconazole/g MCM-41) and the subsequent suspension stirred for 24 hours at room temperature. Then, an excess of N3 (0.4 mL, 1.4 mmol) was added and the mixture was stirred for 5.5 hours at room temperature. The obtained solid was filtered, washed with CH_2Cl_2 (4 mL), and dried under vacuum. Then, this solid was suspended in water at pH 2 (25 mL) in the presence of sulfate for 10 minutes, in order to maintain the gate closed due to amine protonation. The final solid nanodevice loaded with tebuconazole was dried under a vacuum and stored at 37°C for 24 hours.

Yeast preparation for S1-Teb uptake and cell viability assay

Following a similar yeast treatment as for solid nanodevices loaded with FL (S1-FL) assays, BY4741 cells were cultured in yeast peptone dextrose (YPD) medium overnight at 28°C with continuous agitation at a density of 108 cells/mL. Nine milliliters of this suspension was centrifuged for 1 minute at 3,000 rpm and the precipitate was resuspended with 900 µL of simulated vaginal fluid (SVF). Two more washes were done by adding 900 µL of SVF to the previous pellet, and 100 µL of the final cell suspension was introduced in different Eppendorf vials. The SVF was prepared as described by Marques et al.[40] SVF composition in g/L was as follows: sodium chloride 3.51, potassium hydroxide 1.40, calcium hydroxide 0.222, bovine serum albumin 0.018, lactic acid 2.00, acetic acid 1.00, glycerol 0.16, urea 0.40, and glucose 5.00. Then, SVF was adjusted to pH 4.2 with HCl and saved using a sterilized vacuum filtration system.

Results and discussion

Firstly, a material (S1-FL) consisting of mesoporous nanoparticle (MSN) support (MCM-41) loaded with a dye and capped with an organic molecular entity was designed. The starting nanoparticulated MCM-41 mesoporous solid was synthesized following well-known procedures using CTAB as a template and TEOS as a hydrolytic inorganic precursor.[19–24] Then, MCM-41 solid was obtained after calcinations and loaded with the FL dye. As a molecular gate, the organic entity N3, which contains three amine groups per molecule, was selected.

This solid was synthesized, characterized, and tested in vitro (see Supplementary materials for synthesis, characterization, and in vitro results of S1-FL). For the in vitro assays, *S. cerevisiae* cells were incubated in a medium at pH 3.7 with S1-FL at different concentrations (0.65, 1.25, 2.5, and 5 mg/mL) at 40°C for 6 hours. After the heat shock treatment, cells were seeded in plates and incubated for 72 hours. No cell viability differences were found among *S. cerevisiae* cells incubated in regular conditions and the ones incubated at 40°C (data not shown). Moreover, 72 hours is the average time required for yeast colonies to grow up to a size of 1–2 mm, where they can be visually quantitated. Cellular uptake was monitored by fluorescence microscopy (see Supplementary materials).

The cellular uptake of nanoparticles was followed by FL-associated fluorescence (green). The cells incubated at pH 3.7 and treated with S1-FL showed a normal phenotype when compared with control cells. Besides, an FL-associated fluorescence signal was observed, thus proving the internalization and aperture of nanoparticles. In order to rule out any possible toxic effect of nanoparticles under the test conditions, cell viability was monitored throughout the experiments by clonogenic assays. No cell toxicity associated with S1-FL was observed (see Supplementary materials).

After these satisfactory results with S1-FL nanoparticles, we next designed, prepared, characterized, and tested a new material, S1-Teb, as a possible therapeutic antifungal carrier. This nanoparticle design and action mechanism is shown in Figure 1.

Under normal vaginal conditions (Figure 1A), pH remains between 3.8 and 4.4. As a consequence, the molecular gate in S1-Teb material is closed, and no tebuconazole release is produced. Only a few nanoparticles could cross the vaginal epithelium with virtually no toxicity, because tebuconazole's molecular target, encoded by the *lanosterol 14-alpha-demethylase (ERG11)* gene,[41] is not present in human cells. When a *C. albicans* infection occurs in the vaginal environment (Figure 1B), pH is increased (pH >5.5), thus opening the gate and releasing tebuconazole.

Moreover, some of the S1-Teb nanoparticles would be internalized in *C. albicans* (*S. cerevisiae* in our case), where

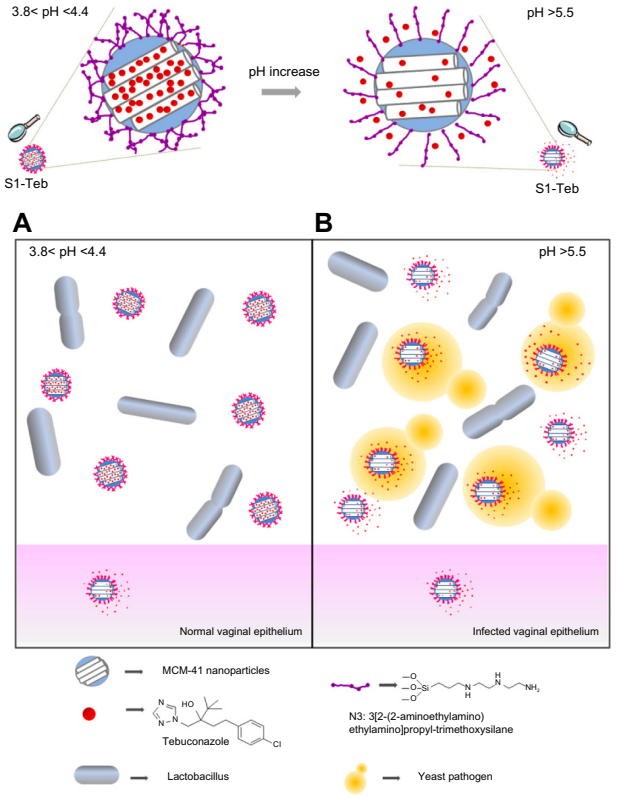

Figure 1 Schematic representation of the design and action mechanism of S1-Teb under usual vaginal conditions (**A**) and in the presence of *Candida albicans* (**B**) (*Saccharomyces cerevisiae* has been used in experimental assays as a model organism).
Abbreviation: MCM-41, mobil composition of matter-41; S1-Teb, MCM-41 loaded with tebuconazole.

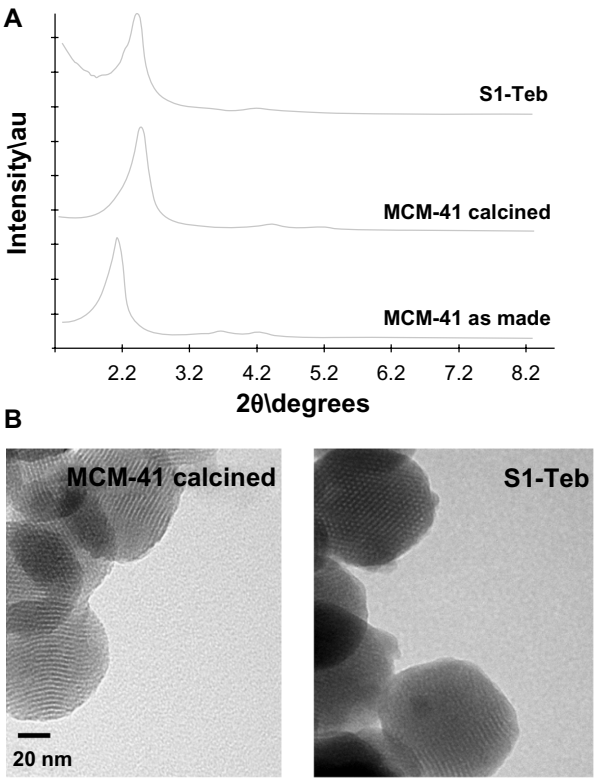

Figure 2 S1-Teb characterization results. (**A**) Powder X-ray pattern of MCM-41 as made, MCM-41 calcined, and S1-Teb. (**B**) Transmission electron microscopy image of MCM-41 calcined and S1-Teb.
Abbreviations: MCM-41, mobil composition of matter-41; S1-Teb, MCM-41 loaded with tebuconazole.

tebuconazole delivery should also occur. Increased lethality of *C. albicans* cells should be expected in this case.

Nanometric mesoporous MCM-41 phase (~100 nm) was selected as inorganic support. MCM-41 nanoparticles were synthesized following the same procedures as for S1-FL[19–24] and obtained after calcination. Then, this calcined material was loaded in this case with tebuconazole, an antifungal drug from the triazoles family whose solubility and size properties resemble those of econazole nitrate.[4] Then, the external surface of the nanoparticles was also functionalized with N3 (see Materials and methods for experiment details).

The MCM-41 structure was confirmed by PXRD and TEM techniques (see Figure 2A and B), which presented the expected features of this type of mesoporous material.

The nitrogen adsorption–desorption isotherms of the prepared phase (see Figure 3A) show a typical Pearson type IV curve with a specific surface area of 998.4 m^2g^{-1}, calculated with the BET[38] model. The absence of a hysteresis loop in this interval and the narrow BJH[39] pore size distribution, with an average pore diameter of 2.45 nm, indicates the existence of uniform cylindrical mesopores with a pore volume of 0.76 cm^3g^{-1}.

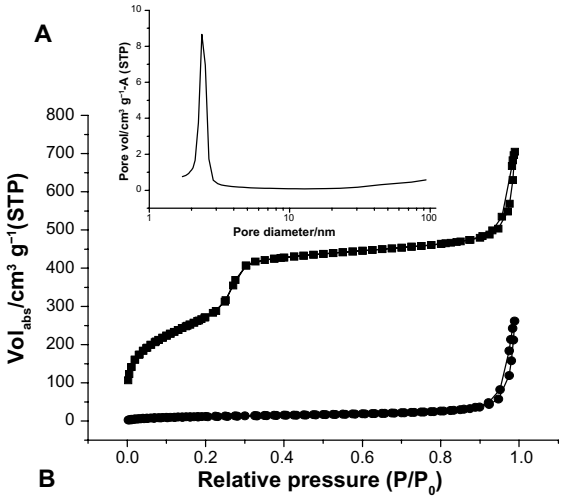

	α_{Teb} (mmol/g SiO_2)	α_{N3} (mmol/g SiO_2)
S1-Teb	0.064	2.43

Figure 3 S1-Teb characterization results. (**A**) Nitrogen adsorption–desorption isotherms of MCM-41 calcined and S1-Teb. (**B**) Contents in mmol/g SiO_2 for S1-Teb. Insets: Pore size distribution of MCM-41 calcined.
Abbreviations: MCM-41, mobil composition of matter-41; STP, standard temperature and pressure; S1-Teb, MCM-41 loaded with tebuconazole.

The prepared solid S1-Teb was also characterized using standard techniques. S1-Teb displays expected characteristics of the MCM-41 phase, as can be observed in the X-ray pattern (Figure 2A) and TEM image in Figure 2B. This suggests that loading and functionalization procedures did not modify the mesoporous structure of the starting material. Additionally, the nitrogen adsorption–desorption isotherm of S1-Teb was typical of gated and filled mesoporous systems, and a significant decrease in the nitrogen volume adsorbed was observed (0.04 cm^3g^{-1}), and in surface area (46.3 m^2g^{-1}), when compared with the starting MCM-41 material (see Figure 3A). Finally, the organic content of the final S1-Teb solid was determined by thermogravimetric and elemental analysis. The amounts of tebuconazole and capping molecule N3 obtained in the final material were 0.064 and 2.43 mmol/g SiO_2, respectively (see Figure 3B).

Yeast uptake and cell viability assay with S1-Teb

Different solutions of free tebuconazole and suspensions of solid S1-Teb with several concentrations (0–200 µg tebuconazole/mL) were prepared by adding dimethyl sulfoxide 2× and SVF at a final volume of 200 µL and 2% dimethyl sulfoxide concentration. The amount of free drug used in the study was the same as that contained in the capped solid S1-Teb, calculated by elemental analysis and thermogravimetry studies (see Supplementary materials). Then, 100 µL of the aforementioned solutions or solid suspensions were added to the different Eppendorf vials containing 100 µL of the yeast suspension (for yeast preparation treatment see Supplementary materials). These final yeast suspensions containing different amounts of free tebuconazole or S1-Teb (0–100 µg tebuconazole/mL) were incubated for 6 hours at 37°C with no stirring. After the incubation period, approximately 300 cells were seeded in a YPD plate and incubated at 28°C for 72 hours. Finally, colony formation units (CFUs) were quantified. The results of the experiments containing duplicates were repeated twice (see Figure 4).

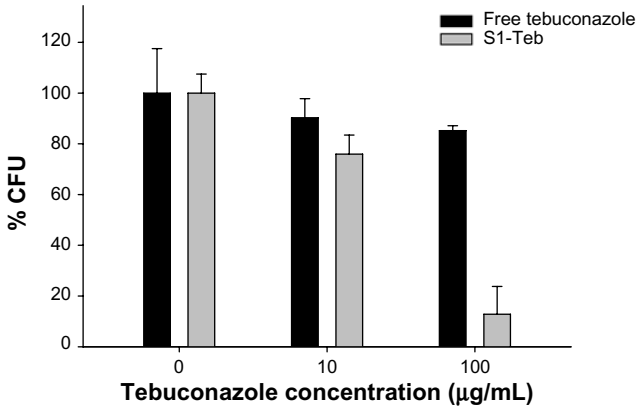

Figure 4 Cell viability assay results of free tebuconazole and S1-Teb in the presence of *Saccharomyces cerevisiae*. Percentage colony formation unit (CFU) growth versus tebuconazole concentration in µg/mL is represented.
Abbreviation: S1-Teb, MCM-41 loaded with tebuconazole.

Satisfactorily, as can be observed, when 100 µg/mL of antifungal is used for both formulations (free and S1-Teb), a very low cell growth value was obtained with the nanoparticles (around 10% CFUs were quantified), whereas most of the cells were grown (around 90% CFUs) with the free antifungal. Practically no significant cell death was achieved with the use of free drug, whereas close to 90% cell death was achieved with S1-Teb.

Conclusion

In summary, a study of the controlled release of different cargo molecules from a mesoporous silica-based material gated with a polyamine able to remain closed at an acidic pH, is described. For the capped solid loaded with FL (S1-FL), in vitro studies showed a selective delivery over 5.5 pH, whereas the molecular gate remains closed at an acidic pH 3.7. Intracellular cargo release and cell viability studies were carried out to analyze the behavior of the solid by employing *S. cerevisiae*, which is a micro-organism that survives in acidic environments, and perfectly suits the aperture mechanism of synthesized nanoparticles. Satisfactorily, S1-FL cell viability studies demonstrated the nontoxicity of the material. Moreover, this solid perfectly internalized in yeast cells, producing the subsequent FL delivery due to the 5.5 pH, as the fluorescence microscopy images demonstrate (see Supplementary materials). In order to demonstrate the potential of this capped material in a therapeutic field as a possible antifungal carrier, other material (S1-Teb) consisting of silica mesoporous support containing an antifungal, tebuconazole, was prepared. Accordingly, a nine-fold increase in tebuconazole cytotoxicity was obtained by using S1-Teb nanoparticles, when compared with that of free antifungal. Therefore, the designed nanoformulation considerably improves tebuconazole efficacy. The enhancement of tebuconazole action could potentially overcome the adverse side effects associated with topical therapies for vulvovaginal infection and significantly improve its cost-effectiveness.

Acknowledgments

The authors thank the Spanish Government (Project MAT2012-38429-C04-01 and Project AGL2012-39597-C02-02), the Generalitat Valenciana (project PROMETEO/2009/016), and the CIBER-BBN for their support. Núria Mas also thanks the Ministerio de Ciencia e Innovación for her FPI grant.

Laura Mondragon thanks the Generalitat Valenciana for her VALI+D post-doctoral fellowship. We dedicate this article to the loving memory of Silvia Hurtado who passed away in September 2013.

Disclosure

The authors report no conflicts of interest in this work.

References

1. Makela P, Leaman D, Sobel JD. Vulvovaginal trichosporonosis. *Infect Dis Obstet Gynecol*. 2003;11:131–133.
2. Edwards L. The diagnosis and treatment of infectious vaginitis. *Dermatol Ther*. 2004;17:102–110.
3. Hainsworth T. Diagnosis and management of candidiasis vaginitis. *Nurs Times*. 2002;98:30.
4. Ambrogi V, Perioli L, Pagano C, et al. Econazole nitrate-loaded MCM-41 for an antifungal topical powder formulation. *J Pharm Sci*. 2010;99:4738–4745.
5. Panácek A, Kolár M, Vecerová R, et al. Antifungal activity of silver nanoparticles against Candida spp. *Biomaterials*. 2009;30:6333–6340.
6. Georgea C, Kuriakosea S, Georgea S, Mathewb T. Antifungal activity of silver nanoparticle-encapsulated β-cyclodextrin against human opportunistic pathogens. *Supramolecular Chem*. 2011;23:593–597.
7. Paulo CSO, Vidal M, Ferreira LS. Antifungal nanoparticles and surfaces. *Biomacromolecules*. 2010;11:2810–2817.
8. Saha S, Leung KCF, Nguyen TD, Stoddart JF, Zink JI. Nanovalves. *Adv Func Mater*. 2007;17:685–693.
9. Trewyn BG, Slowing II, Giri S, Chen HT, Lin VSY. Synthesis and functionalization of a mesoporous silica nanoparticle based on the sol-gel process and applications in controlled release. *Acc Chem Res*. 2007;40:846–853.
10. Coll C, Bernardos A, Martínez-Máñez R, Sancenón F. Gated silica mesoporous supports for controlled release and signaling applications. *Acc Chem Res*. 2013;46:339–349.
11. Yang P, Gai S, Lin J. Functionalized mesoporous silica materials for controlled drug delivery. *Chem Soc Rev*. 2012;41:3679–3698.
12. Li Z, Barnes JC, Bosoy A, Stoddart JF, Zink JI. Mesoporous silica nanoparticles in biomedical applications. *Chem Soc Rev*. 2012;41:2590–2605.
13. Mal NK, Fujiwara M, Tanaka Y. Photocontrolled reversible release of guest molecules from coumarin-modified mesoporous silica. *Nature*. 2003;421:350–353.
14. Schlossbauer A, Kecht J, Bein T. Biotin-avidin as a protease-responsive cap system for controlled guest release from colloidal mesoporous silica. *Angew Chem In. Ed*. 2009;48:3092–3095.
15. Thornton PD, Heise A. Highly specific dual enzyme-mediated payload release from peptide-coated silica particles. *J Am Chem Soc*. 2010;132:2024–2028.
16. Park C, Kim H, Kim S, Kim C. Enzyme responsive nanocontainers with cyclodextrin gatekeepers and synergistic effects in release of guests. *J Am Chem Soc*. 2009;131:16614–16615.
17. Liu R, Zhao X, Wu T, Feng P. Tunable redox-responsive hybrid nanogated ensembles. *J Am Chem Soc.* 2008;130:14418–14419.
18. Aznar E, Martínez-Máñez R, Sancenón F. Controlled release using mesoporous materials containing gate -like scaffoldings. *Expert Opin Drug Deliv*. 2009;6:643–655.
19. El Haskouri J, Ortiz de Zarate D, Guillem C, et al. Silica-based powders and monoliths with bimodal pore systems. *Chem Commun*. 2002;4:330–331.
20. Comes M, Marcos MD, Martínez-Máñez R, et al. Chromogenic discrimination of primary aliphatic amines in water with functionalized mesoporous silica. *Adv Mater*. 2004;16:1783–1786.
21. Comes M, Rodríguez-López G, Marcos MD, et al. Host solids containing nanoscale anion-binding pockets and their use in selective sensing displacement assays. *Angew Chem Int Ed*. 2005;44:2918–2922.
22. Kresge CT, Leonowicz ME, Roth WJ, Vartuli JC, Beck JS. Ordered mesoporous molecular sieves synthesized by a liquid-crystal template mechanism. *Nature*. 1992;359:710–712.
23. Rámila A, Muñoz B, Pérez-Pariente J, Vallet-Regí M. Mesoporous MCM-41 as drug host system. *J Sol-Gel Sci Technol*. 2003;26:1199–1202.
24. Vallet-Regí M. Ordered mesoporous materials in the context of drug delivery systems and bone tissue engineering. *Chem Eur J*. 2006;12:5934–5943.
25. Vadia N, Rajput S. Mesoporous material, MCM41: a new drug carrier. *Asian J Pharm Clin Res*. 2011;4:44–53.
26. Beck JS, Vartuli JC, Roth WJ, et al. A new family of mesoporous molecular sieves prepared with liquid crystal templates. *J Am Chem Soc*. 1992;114:10834–10843.
27. Wright AP, Davis ME. Design and preparation of organic–inorganic hybrid catalysts. *Chem Rev*. 2002;102:3589–3614.
28. Kickelbick G. Hybrid inorganic–organic mesoporous materials. *Angew Chem Int Ed*. 2004;43:3102–3104.
29. Lai C-Y, Trewyn BG, Jeftinija DM, et al. A mesoporous silica nanosphere-based carrier system 373 with chemically removable CDS nanoparticle caps for stimuli-responsive 374 controlled release of neurotransmitters and drug molecules. *J Am Chem Soc*. 2003;125: 4451–4459.
30. Doadrio AL, Doadrio JC, Sánchez-Montero JM, Salinas JA, Vallet-Regí M. A rational explanation of the vancomycin release from SBA-15 and its derivative by molecular modeling. *Micropor Mesopor Mater*. 2010;132:559–566.
31. Molina-Manso D, Manzano M, Doadrio JC, et al. Usefulness of SBA-15 mesoporous ceramics as a delivery system for vancomycin, rifampicin and linezolid: a preliminary report. *Int J Antimicrob Agents*. 2012;40:252–256.
32. Mellaerts R, Aerts CA, Humbeeck JV, Augustijns P, Van den Mooter G, Martens JA. Enhanced release of itraconazole from ordered mesoporous SBA-15 silica materials. *Chem Commun (Camb)*. 2007;13:1375–1377.
33. Premanathan M, Amaar Shakurfow FA, Ismail AA, Berfad MA, Ebrahim AT, Awaj MM. Treatment of oral candidiasis (thrush) by Saccharomyces cerevisiae. *Int J Med Med Sci*. 2011;3:83–86.
34. Homann OR, Dea J, Noble SM, Johnson AD. A phenotypic profile of the Candida albicans regulatory network. *PLOS Genetics*. 2009;5: 1–12.
35. Shaw W. Yeast and fungi. How to control them. *Biological Treatments for Autism and PDD*. 3rd ed. Lenexa, KS: Great Plains Laboratory Inc.; 2008.
36. Casasús R, Marcos MD, Martínez-Máñez R, et al. Toward the development of ionically controlled nanoscopic molecular gates. *J Am Chem Soc*. 2004;126:8612–8613.
37. Casasús R, Climent E, Marcos MD, et al. Dual aperture control on pH- and anion-driven supramolecular nanoscopic hybrid gate-like ensembles. *J Am Chem Soc*. 2008;130:1903–1917.
38. Brunauer S, Emmett PH, Teller E. Adsorption of gases in multimolecular layers. Adsorption of gases in multimolecular layers. *J Am Chem Soc.* 1938;60:309–319.
39. Barret EP, Joyner L-G, Halenda PP. The determination of pore volume and area distributions in porous substance. I. Computations from nitrogen isotherm. *J Am Chem Soc*. 1951;73:373–380.
40. Marques MRC, Loebenberg R, Almukainzi M. Simulated biological fluids with possible application in dissolution testing. *Dissolut Technol.* 2011;18:15–28.
41. Song JL, Harry JB, Eastman RT, Oliver BG, White TC. The Candida albicans lanosterol 14-alpha-demethylase (ERG11) gene promoter is maximally induced after prolonged growth with antifungal drugs. *Antimicrob Agents Chemother*. 2004;48:1136–1144.

Supplementary materials

Synthesis of S1-FL

In a typical synthesis, template-free MCM-41 (mobil composition of matter-41) (100 mg) and fluorescein (FL) (16.8 mg, 0.007 mmol) were suspended in methanol (40 mL) inside a round-bottomed flask in an inert atmosphere. The mixture was stirred for 24 hours at room temperature in order to achieve maximum loading in the pores of the MCM-41 scaffolding. Then, an excess of 3-[2-(2-aminoethylamino) ethylamino]propyltrimethoxysilane (N3) (0.2 mL, 0.7 mmol) was added and the final mixture was stirred for 5.5 hours at room temperature. Finally, the solid (nanodevice loaded with fluorescein [S1-FL]) was filtered and washed with methanol (40 mL). Once it was dried, the solid was suspended in water at pH 2 in the presence of sulfate (at this pH, the molecular gate is closed) in order to remove the dye remaining outside the pores. After 12 hours, the solid was filtered and dried at 37°C for 24 hours.

S1-FL characterization

Synthesized material S1-FL was characterized by standard techniques. Figure S1A shows the powder X-ray diffraction (PXRD) patterns of solids MCM-41 as synthesized, MCM-41 calcined, and S1-FL. The PXRD of the mesoporous MCM-41 as synthesized material (curve [a]) showed four peaks, which are typical of a hexagonal ordered array, indexed as (100), (110), (200), and (210) Bragg reflexions. From the PXRD data, an a0 cell parameter of 2.27 Å was calculated. In curve (b) (the MCM-41 calcined sample), an important shift of the (100) to larger angles in PXRD and a broadening of the (110) and (200) reflections were clearly found and attributed to the condensation of the silanol groups in the calcination step. Figure S1 also depicts the PXRD pattern for solid S1-FL. For this material, reflections (110) and (200) were almost lost, probably due to diminished contrast as a result of the loading and functionalization process. Nevertheless, the clear presence in S1-FL of the d100 peak in the XRD patterns supports that pore loading, and the additional functionalization with the amine derivative did not modify the mesoporous structure of the starting MCM-41 scaffolding.

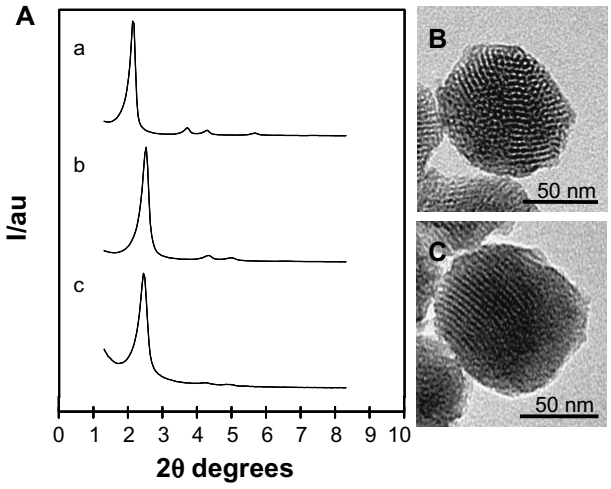

Figure S1 (**A**) The powder X-ray diffraction patterns of the solids (**a**) MCM-41 as synthesized, (**b**) calcined MCM-41, and (**c**) solid nanodevice loaded with fluorescein (S1-FL) containing FL dye and 3-[2-(2-aminoethylamino)ethylamino]propyltrimethoxysilane. The transmission electron microscopy images of (**B**) the calcined MCM-41 sample and (**C**) S1-FL showing the typical porosity of the MCM-41 mesoporous matrix.
Abbreviations: MCM-41, mobil composition of matter-41; I/au, intensity/arbitrary units.

Preservation of the mesoporous structure in both the calcined MCM-41 material and the final functionalized solid S1-FL was also confirmed by means of the transmission electron microscopy images. In both solids, the characteristic channels of a mesoporous matrix were observed as alternate black and white lines. Figure S1B shows the morphology of the prepared mesoporous MCM-41 and S1-FL materials as spherical nanoparticles with a mean diameter of ~100 nm.

In order to complement the information provided by the X-ray and the transmission electron microscopy analyses, porosimetry studies for the MCM-41 calcined material and the final S1-FL materials were carried out (Table S1). The nitrogen adsorption–desorption isotherms of the nanoparticulated MCM-41 calcined material are shown in Figure S2A. A typical curve for these mesoporous solids, consisting of an adsorption step at an intermediate P/P_0 value (0.1–0.3), is observed. The absence of a hysteresis loop in this interval and the narrow BJH pore distribution suggest the existence of uniform cylindrical mesopores (pore diameter of 3.09 nm and pore volume of 0.935 $cm^3\ g^{-1}$ calculated by the BJH model on the adsorption branch of the isotherm). The application of the BET model resulted in a value of 1096 m^2/g for the total specific surface. For S1-FL, the nitrogen adsorption–desorption isotherm (Figure S2) presented the typical characteristics of a mesoporous system with partially filled mesopores. Therefore, lower nitrogen adsorbed volume (BJH mesopore volume =0.482 $cm^3\ g^{-1}$) and surface area (424 m^2/g) values were calculated. Despite the significant drop in

Table S1 BET specific surface values, pore volumes, and pore sizes calculated from the nitrogen adsorption–desorption isotherms for selected materials

	S_{BET} ($m^2\ g^{-1}$)	Pore volume ($cm^3\ g^{-1}$)	Pore size (nm)
MCM-41	1,097	0.94	3.09
S1-FL	424	0.48	3.49

Abbreviations: S1-FL, nanodevice loaded with fluorescein; MCM-41, mobil composition of matter-41; BET, Brunauer–Emmett–Teller theory.

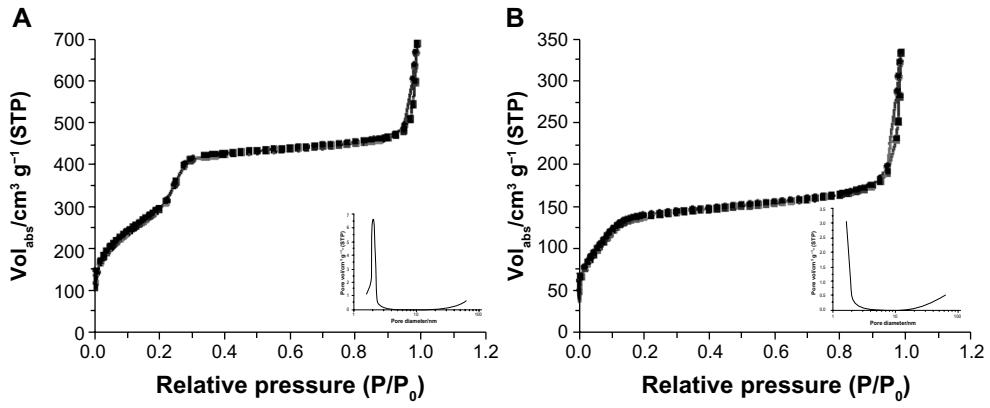

Figure S2 Nitrogen adsorption–desorption isotherms for (**A**) MCM-41 mesoporous material, (**B**) nanodevice loaded with fluorescein (S1-FL). Inset: pore size distribution of the MCM-41 mesoporous material and of S1-FL solid.
Abbreviations: MCM-41, mobil composition of matter-41; Vol_{abs}, volume of nitrogen absorption; STP, standard temperature and pressure.

pore volume, some features were still observed in the BJH mesopore size distribution, such as a maximum at ~1.8 nm (on the border between mesopores and micropores).

Having determined the structure of the nanoparticles synthesized, the amount of guest molecule and N3 on solid S1-FL was determined by thermogravimetric analysis. Table S2 offers the results obtained.

Release kinetics of S1-FL

In order to check the proper aperture mechanism of solid S1-FL, 10 mg was suspended in 25 mL of water containing sulfate anions at a final concentration of 0.01 M at different pH (3.7 and 5.5). Suspensions were stirred at room temperature and, at a given time, aliquots were separated and filtered. The delivery of FL from the pore voids to the aqueous solution was monitored via its fluorescence emission band at 517 nm (λ_{ex}=494 nm). Due to the influence of pH on the fluorescence of FL, all the taken aliquots were treated with the amount of NaOH required to increase their pH to 8.

The dye delivery at different pH is depicted in Figure S3. At the more acidic pH of 3.7, S1-FL was tightly capped and displayed no significant FL release. In contrast, at pH 5.5, the cargo molecule was released. The interpretation of such behavior lies in the different degrees of protonation of amines at different pH values and in the interaction of protonated amines with certain anions. Despite the fact that these p*K*a (acid dissociation logarithmic constant) values can be modified when a number of polyamines are anchored onto the silica surface, it is clear that at pH 3.7, amines become more protonated than at pH 5.5. It has been reported that when protonated, tethered open-chain polyamines tend to adopt a rigid-like conformation that pushes them toward the pore openings.[1] This results in a pore blockage that partially inhibits the dye release. A second effect is related to the interaction of protonated amines with anions (in our case, sulfate). This is based on the capacity that polyamines have to coordinate anionic species. Polyamines have thus been extensively explored as a suitable group for designing abiotic ligands for inorganic and biologically important anionic guests. Amine-containing receptors are polycations (polyammonium ligands), especially at an acidic pH, and they bind anionic species via hydrogen bonding and Coulomb forces. At pH 5.5 and pH 3.7, a combination of both ammonium and amine groups anchored onto the S1-FL surface is expected to occur, where the percentage of ammonium groups grows as

Table S2 Content (α) in mmol of 3-[2-(2-aminoethylamino) ethylamino]propyltrimethoxysilane (N3) and dye per gram of SiO_2 for nanodevice loaded with fluorescein (S1-FL)

Solid	α_{N3}	α_{FL}
S1-FL	0.549	0.376

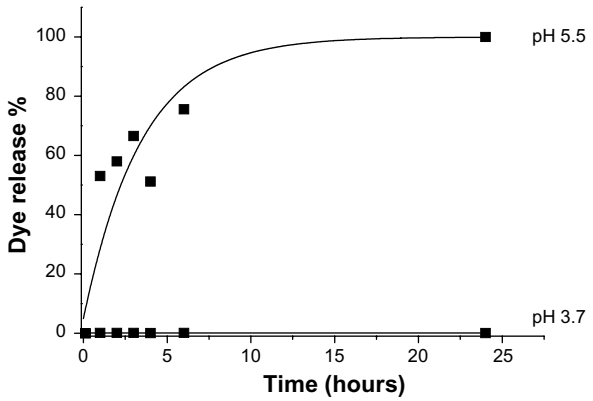

Figure S3 Kinetic release of fluorescein (FL) from solid nanodevice loaded with FL (S1-FL) at pH 3.7 and pH 5.5.

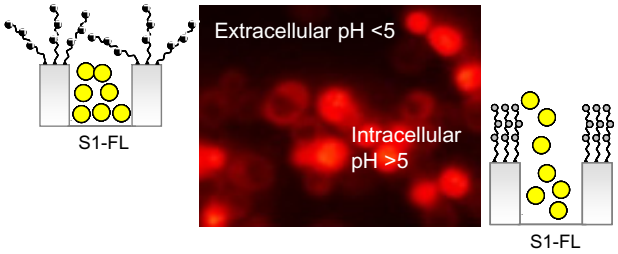

Figure S4 Schematic representation of the hybrid system nanodevice loaded with fluorescein (S1-FL) performance.

pH lowers. For the correct interpretation of the interaction of sulfate with the anchored polyamines, it is important to note that sulfate shows a logarithm for its first protonation of 1.9, indicating that at pH 3.7 and pH 5.5, sulfate acts like SO_4^{2-} species. The observed behavior (ie, sulfate is able to close the gate at pH 3.7 but is unable to inhibit dye release at pH 5.5) can be explained, bearing in mind the larger proportion of positively charged ammonium groups at pH 3.7, which results in a larger electrostatic interaction with sulfate anions. Nevertheless, hydrogen-bonding interactions between the amine/ammonium groups and sulfate cannot be ruled out, as SO_4^{2-} can act as a hydrogen bond acceptor, whereas amines/ammonium groups can behave as hydrogen bond donors.[2]

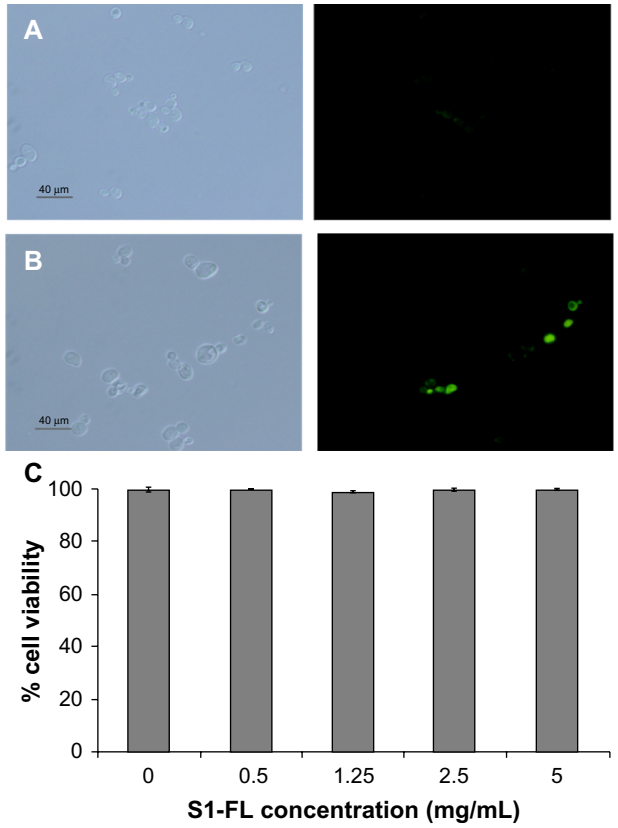

Figure S5 Nanodevice loaded with fluorescein (S1-FL) internalization and cell viability assays. Fluorescence microscopy images corresponding to the *Saccharomyces cerevisiae* cells treated with 5 mg/mL of solids (**A**) MCM-41 and (**B**) S1-FL and incubated at 40°C for 6 hours. The cellular internalization of solid S1-FL was followed by fluorescein-associated fluorescence (green). For the clonogenic cell survival assays (**C**), *S. cerevisiae* cells were treated with 5, 2.5, 1.25, and 0.65 mg/mL of S1-FL. Two independent experiments were performed and data are reported as mean ± standard error of the mean.
Abbreviation: MCM-41, mobil composition of matter-41.

Yeast uptake of S1-FL

We next tested the applicability of mesoporous nanoparticle (MSN) supports based on MCM-41 as nanocarriers for intracellular release in *Saccharomyces cerevisiae*. Our hypothesis was based on the fact that the designed nanoparticle presents zero release of the cargo molecule in acidic environments (at a pH of around 3–4) in the presence of sulfate, in which yeasts are able to grow. Having internalized the solid, the lower acidity inside *S. cerevisiae* (pH 5.5), where the nanoparticles will be located, allows the entrapped molecule to be released (see Figure S4).

The conditions for nanoparticle internalization in yeast cells were then optimized. We first focused on determining the optimal incubation temperature of *S. cerevisiae* cells with nanoparticles and the different agitation rates of cultures. Three different temperatures were tested: 30°C, 37°C, and 40°C. Consequently, 40°C proved the most efficient temperature for nanoparticle uptake, probably due to the increased plasmatic membrane permeability at higher temperatures. Then, internalization and cell viability assays were carried out with S1-FL at 40°C (see Figure S5). When different agitation rates were chosen, no agitation proved optimal for the cellular uptake of solids.

References

1. Bernardos A, Aznar E, Coll C. Controlled release of vitamin B2 using mesoporous materials functionalized with amine-bearing gate-like scaffoldings. *J Control Release*. 2008;131(3):181–189.
2. Song SW, Hidajat K, Kawi S. pH-controllable drug release using hydrogel encapsulated mesoporous silica. *Chem Comm*. 2007;42:4396–4398.